

Freezing molecules with light: How long can one maintain a non-equilibrium molecular geometry by strong light-matter coupling?

Eric R. Bittner,^{1, a)} Ravyn A. Malatesta,² Gabrielle D. Olinger,³ and Carlos Silva-Acuña^{2, 4}

¹⁾Department of Chemistry, University of Houston, Houston, TX 77204

²⁾School of Chemistry and Biochemistry, Georgia Institute of Technology, 901 Atlantic Drive, Atlanta, GA 30332

³⁾Department of Physics, University of Houston, Houston, TX 77204

⁴⁾School of Physics, Georgia Institute of Technology, 837 State Street, Atlanta, GA 30332

(Dated: 21 April 2021)

In molecular photochemistry, the non-equilibrium character and subsequent ultrafast relaxation dynamics of photoexcitations near the Franck-Condon region limit the control of their chemical reactivity. We address how to harness strong light-matter coupling in optical microcavities to isolate and preferentially select specific reaction pathways out of the myriad of possibilities present in large-scale complex systems. Using Fermi's Golden Rule and realistic molecular parameters, we estimate the extent to which molecular configurations can be "locked" into non-equilibrium excited state configurations for timescales well beyond their natural relaxation times. For upper polaritons—which are largely excitonic in character, molecular systems can be locked into their ground state geometries for tens to thousands of picoseconds and varies with the strength of the exciton/phonon coupling (Huang-Rhys parameter). On the other hand, relaxed LP lifetimes are nearly uniformly distributed between 2.1 – 2.4 ps and are nearly independent of the Huang-Rhys parameter.

I. INTRODUCTION

The past few years has seen a remarkable surge in the use and application of photonic optical cavities to induce, manipulate, and modify chemical process through strong coupling between quantized cavity photons and molecular states to form polaritons.^{1–6} Cavity polaritons arise from non-perturbative coupling between the strongly quantized modes of the electromagnetic fields in the optical cavity and the optical transitions of the molecular species within the cavity. These transitions can be vibrational or vibronic depending upon the tuning of the cavity.

In the absence of a cavity, the electronic transitions can be described within a Franck-Condon description whereby optical transitions from the ground state to the excited state occur within a fixed nuclear frame; this is followed by relaxation/reorganization on the excited state potential to some new local minimum energy geometry and then fluorescence or non-radiative decay carries the system back to the ground state. Generally, the reorganization occurs on a timescale on the order of ps, fluorescence occurs on the order of ns, and non-radiative decay occurs on timescales the order of ns to ms. As a result, fluorescence occurs according to Kasha's rule from the lowest lying vibronic state of the excited state potential to the ground state potential that gives rise to the vibronic fine structure readily observed these systems. There may also be other important intersystem processes competing with this, such as charge-transfer and other photophysical processes that are initiated by the relaxation from the Franck-Condon point.

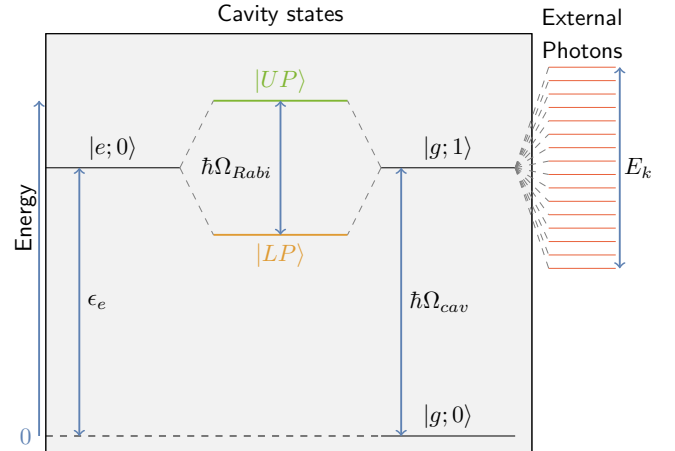


FIG. 1. Energy level diagram depicting the electronic and photon excitations in the microcavity.

In a microcavity, this picture needs to be modified in number of important ways.^{7–11} First, the correct quantum mechanics basis includes the quantized radiation field states into the atomic or molecular basis. We denote these as $|\phi; n_k\rangle$ where ϕ denotes the material (atomic, molecular, etc.) state while n_k denotes the number of quanta (photons) in the k -th mode of the radiation field. Thus, a molecule in the ground state with a cavity devoid of photons would be denoted as $|g; 0_k\rangle$ with energy $E_g + \hbar\omega_k$. This is depicted in Fig.2 in which to a first approximation the electronic potential surfaces are vertically shifted in energy by $\hbar\omega_k n_k$. For clarity, we show the case for a single mode cavity with frequency ω_c . If the cavity is resonant or nearly resonant with the optical transition frequency, ω_x , the adiabatic potential for the $|g; n_k\rangle$ (*i.e.* molecular ground state + n_k cavity pho-

^{a)}Electronic mail: ebittner@central.uh.edu

tons) intersects the potential for the $|e; (n_k - 1)\rangle$ (*i.e.* molecular excited state + $n_k - 1$ cavity photons) near the Franck-Condon point. Coupling between the radiation field and the atomic or molecule state, introduces a new set of eigenstates of the matter/radiation field which are linear combinations of the dressed-atom states termed lower (LP) and upper (UP) polaritons.

$$\begin{pmatrix} |L_k(n_k)\rangle \\ |U_k(n_k)\rangle \end{pmatrix} = \begin{bmatrix} c_k & s_k \\ -s_k & c_k \end{bmatrix} \begin{pmatrix} |g; n_k\rangle \\ |e; (n_k - 1)\rangle \end{pmatrix} \quad (1)$$

with coefficients $c_k^2 + s_k^2 = 1$. At the crossing point, the two states are split by the Rabi frequency $\hbar\Omega_{Rabi} = 2|\mu_{eg}|\sqrt{n_k}E_k$ where $E_k = \sqrt{\hbar\omega_k/2\epsilon V_{cav}}$ is the electric field of the cavity (assuming optimal alignment between the molecular transition moments and the electric field in the cavity and cavity permittivity ϵ and volume V_{cav}).

A second but equally important consideration is that the eigenstates of the cavity (the polariton states) are embedded in a continuum of photon states exterior to the cavity which “dress” the cavity states.¹² Within this picture, sketched in Fig. 1, each polariton state, ϕ , is embedded into the continuum by writing it as

$$|\psi_\mu\rangle = \sum_\phi c_\phi |\phi\rangle + \sum_n c_n |n\rangle. \quad (2)$$

These are formally eigenstates of a Schrödinger equation $(H_{cav} + H_{ext} + \hat{W})|\psi_\mu\rangle = E_\mu|\psi_\mu\rangle$ where H_{cav} is the cavity Hamiltonian with eigenstates $|\phi\rangle$ with energies E_ϕ . H_{ext} is the Hamiltonian for a quasi-continuum of external states $|n\rangle$ with energy $E_n = n\delta$, respectively. Here, integer $n \in (-\infty, \infty)$ indexes the quasi-continuum states with uniform spacing δ . Our final results will require $\delta \rightarrow 0$.

We write \hat{W} as the coupling between the internal (cavity) and external states. An initially prepared interior (cavity) state will decay exponentially into the quasi-continuum of external states with time constant Γ_ϕ as per Fermi’s golden rule (FGR)

$$\Gamma_\phi = \frac{2\pi}{\hbar} |\langle \psi_\mu | \hat{W} | \phi \rangle|^2 \frac{1}{\delta} \quad (3)$$

where $\delta \rightarrow 0$ is the spacing between the quasi-continuum states exterior to the cavity.

Ordinarily, the UP and LP decay rates are “inherited” from the properties of the cavity and can be written as a weighted sum of the exciton decay rate and the cavity leakage rate

$$\Gamma_{lp} = |s_k|^2 \Gamma_{ex} + |c_k|^2 \Gamma_{cav} \quad (4)$$

This implies that the lower polariton lifetime is set by the fastest decaying component which is generally the lifetime of a photon in the cavity. However, experimental studies of organic microcavity systems suggest that their polariton states are much longer lived.^{13–15} This can be explained within the exciton bath-model developed by Lidsey et al, the kinetics of populating the lower

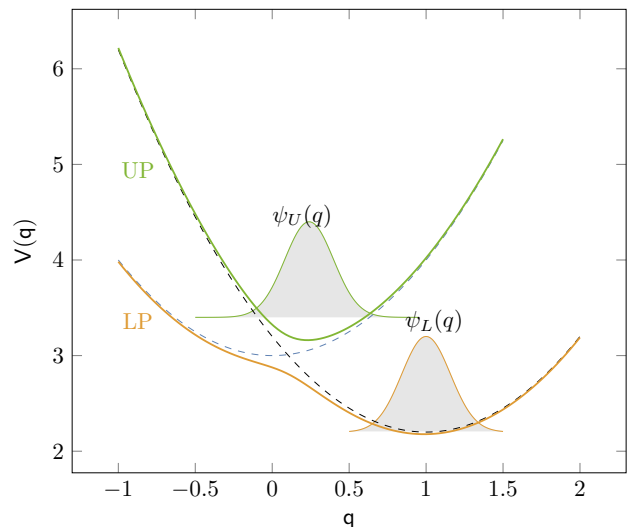


FIG. 2. Schematic potential surfaces for a molecular system interacting with a single-mode cavity.

(emissive) polariton state is slow compared to its emission rate.¹⁶ Furthermore, the observed emission rates are not angle dependent, suggesting that there is sufficient thermalization of the cavity states.

Of central concern of this paper is the cavity induced (or suppressed) dynamics of the molecular species on the UL and LP adiabatic potentials and importantly, the non-adiabatic coupling between the two. Vibrational and nuclear motions about and away from this point introduce coupling between the UP and LP states. In other words, the light-matter coupling introduces a non-adiabatic coupling between UP and LP adiabatic potentials. This non-adiabatic coupling affects the lifetime of molecular polaritons. The relaxed exciton is decoupled from the cavity and population in this state serves as a “dark reservoir”.

In this paper we use Fermi’s golden rule (FGR) to compute the both UP and LP lifetimes using a vibronic coupling model. First, we will work with a exciton/phonon model that incorporates on- and off-diagonal couplings between the electronic terms and the internal vibrational modes of the molecular system. We append to this the coupling between the electronic terms and the cavity photon modes within the Tavis-Cummings model. We use this as the starting point for computing the non-adiabatic coupling between the UP and LP polariton adiabatic potentials due to the vibronic motions of the molecule on these potentials. We arrive at simple expressions based upon the molecular vibronic couplings and frequencies and use this to estimate UP to LP conversion times for a wide range of molecular chromophore systems.

II. VIBRONIC COUPLING BETWEEN POLARITON BRANCHES

To frame our discussion, we use the following exciton/phonon model Hamiltonian

$$H_{ex} = \sum_i \epsilon_i |i\rangle\langle i| + \sum_{ijq} g_{ijq} (|i\rangle\langle j| + |j\rangle\langle i|) (\hat{b}_q^\dagger + \hat{b}_q) + \sum_q \hbar\omega_q \hat{b}_q^\dagger \hat{b}_q \quad (5)$$

where ϵ_i are the electronic energies referenced to common molecular geometry (e.g. the ground state, $i = 0$, and excited states $i > 0$), g_{ijq} are the diagonal and off-diagonal derivatives of the potential at this geometry, and $[\hat{b}_q, \hat{b}_{q'}^\dagger] = \delta_{qq'}$ are boson operators for vibrational phonon modes with frequency ω_q . Each of these parameters can be determined by quantum chemical means.¹⁷⁻²⁷ Importantly, the ϵ_i energies correspond to the electronic eigenenergies *defined* at some local energy minimum. Correspondingly, the phonon normal modes, frequencies $\hbar\omega_q$, and coupling forces g_{ijq} are similarly defined relative to this configuration. We append to this the radiation modes of a microcavity and couplings within the Tavis/Cummings model²⁸

$$\hat{V}_{cav} = \sum_k \hbar\Omega_{k,cav} \hat{a}_k^\dagger \hat{a}_k + \sum_{k,i>0} \mu_{i0} E_o (|0\rangle\langle i| \hat{a}_k^\dagger + |i\rangle\langle 0| \hat{a}_k) \quad (6)$$

where we take $\mu_{i0} E_o$ to be the projection of the transition moment between the ground and excited states onto the electric field in the cavity. We assume the cavity has a single mode that is nearly resonant with a single electronic transition and work within a dressed-atom basis and write $|0\rangle = |g, 1_k\rangle$ as the electronic ground-state with 1_k cavity photons and $|1\rangle = |e, 0_k\rangle$ as the first exciton state with 0_k cavity photons.

Fig.2 is a sketch of the adiabatic potentials for molecular motions in the UP and LP eigenbasis. The dashed (diabatic) potentials correspond to the diabatic potentials for the ground and excited molecular states; however, the ground state potential is shifted up by the energy of a single cavity photon. In the scenario shown here, the cavity is resonant with the absorption frequency of the molecule. Vibrational wavepacket dynamics then follow the lower (orange) adiabatic potential away from the Franck-Condon point. As the molecule distorts along coordinate q , the resulting polariton state evolves from being a 1:1 linear combination of a cavity photon and molecular excitation to being purely excitonic by the time it has relaxed.

Transforming to the UP/LP basis and assuming the cavity contains a single excitation, the cavity Hamiltonian takes the form

$$\begin{aligned} \tilde{H}_{cav} &= H_{ex} + V_{cav} \\ &= \begin{pmatrix} \hat{L}_k^\dagger & \hat{U}_k^\dagger \end{pmatrix} \cdot \begin{bmatrix} \hbar\Omega_{L,k} + (s_k^2 g_1 - 2c_k s_k g_{01}) \cdot X & (g_{01}(c_k^2 - s_k^2) - c_k s_k g_1) \cdot X \\ (g_{01}(c_k^2 - s_k^2) - c_k s_k g_1) \cdot X & \hbar\Omega_{U,k} + (c_k^2 g_1 + 2c_k s_k g_{01}) \cdot X \end{bmatrix} \cdot \begin{pmatrix} \hat{L}_k \\ \hat{U}_k \end{pmatrix} + \hbar\Omega \hat{B}^\dagger \hat{B} \\ &= \begin{pmatrix} \hat{L}_k^\dagger & \hat{U}_k^\dagger \end{pmatrix} \left[\begin{bmatrix} \hbar\Omega_{L,k} & 0 \\ 0 & \hbar\Omega_{U,k} \end{bmatrix} + \begin{bmatrix} G_L & G_{LU} \\ G_{UL} & G_U \end{bmatrix} \cdot (B + B^\dagger) \right] \begin{pmatrix} \hat{L}_k \\ \hat{U}_k \end{pmatrix} + \hbar\Omega \hat{B}^\dagger \hat{B}, \end{aligned} \quad (7)$$

where the coefficients G_L , G_U , and G_{UL} contain contributions from both the cavity and the original (cavity free) electron/phonon coupling. The G_L and G_U will introduce a reorganization energy to both the UP and LP potential surfaces while the G_{LU} and G_{UL} terms couple the UP and LP polariton branches via both diagonal and off-diagonal exciton/phonon coupling terms. This generalized model can be parameterized from *ab initio* calculations.

A. Reduced Model

To analyse the interplay between the internal degrees of freedom and the cavity, we consider a far simpler model of a two-electronic state molecule with a single vibrational degree of freedom with frequency ω

$$H_{ex} = \epsilon_g |g\rangle\langle g| + |e\rangle\langle e| (\epsilon_e + \hbar\omega S (b^\dagger + b)) + g_{eg} (|g\rangle\langle e| + |e\rangle\langle g|) (b^\dagger + b) + \hbar\omega b^\dagger b. \quad (8)$$

Here, S is a dimensionless (Huang-Rhys) parameter that determines the relative shift between the ground state potential and the excited state diabatic potentials. Under this simplified model,

$$G_L = \sin(\eta)^2 \hbar\omega S - 2g_{eg} \sin(2\eta) \quad (9)$$

$$G_U = \cos(\eta)^2 \hbar\omega S + 2g_{eg} \sin(2\eta) \quad (10)$$

$$G_{LU} = g_{eg} \cos(2\eta) - \hbar\omega S \sin(2\eta)/2 \quad (11)$$

where

$$\frac{1}{2} \tan(2\eta) = -\frac{\lambda_{eg}}{(\epsilon_e - \epsilon_g) - \hbar\Omega_{cav}} \quad (12)$$

defines the mixing between the electronic transition between $|g\rangle$ and $|e\rangle$ and the photon mode of the cavity and $\lambda_{eg} = \mu_{eg} E_o \sqrt{n_k}$ includes the molecular transition moment, field, and mode occupancy n_k .

B. Embedding into the continuum

Thus far, we have neglected the dressing of the cavity states (i.e. the UP and LP polaritons) by their coupling \hat{W} to the photon states which are external to the cavity. For this, we apply the approach developed in Ref. 12 whereby we write $|\psi_\mu\rangle$ as a solution of the full cavity + continuum Schrödinger equation

$$(\hat{H}_{cav} + H_{ext} + \hat{W})|\psi_\mu\rangle = E_\mu|\psi_\mu\rangle \quad (13)$$

Accordingly, we define the following matrix elements:

$$v_n = \langle n|\hat{W}|LP\rangle = v \quad (14)$$

$$v'_n = \langle n|\hat{W}|UP\rangle = v' \quad (15)$$

$$0 = \langle n|\hat{W}|n'\rangle = \langle n|H_{ext}|LP\rangle = \langle n|H_{ext}|UP\rangle \quad (16)$$

Direct (phonon mediated) coupling between the UP and LP is mediated by the off-diagonal terms in Eq.7 and Eq.8. For compactness in notation and to parallel the development in Ref.¹² we shall write

$$\hat{w} = G_{LU}(b^\dagger + b) \quad (17)$$

and recognize that we will need to average over the initial vibrational states to obtain our final expressions.

C. Why Eq. 4 is incomplete

The assumption that the polariton decay is dictated by the cavity lifetime can be analyzed using the FGR approach. However, rather than using the vibronic coupling (as suggested above) as the perturbation, we take the light-matter interaction as the perturbation and consider the decay of the molecular excitation $|e; 0\rangle$ into the quasi-continuum. The FGR rate for the exciton decay is then given by

$$\Gamma_{ex} = \frac{2\pi}{\hbar} |\langle \psi_\mu | \hat{W} | e; 0 \rangle|^2 \frac{1}{\delta}. \quad (18)$$

If we assume that the decay of $|e; 0\rangle$ is via $|g; 1\rangle$, which in turn can decay to $|g; 0\rangle$ by photon leakage from the cavity, then the coupling between the exciton and the continuum is given by

$$\langle \psi_\mu | \hat{W} | e; 0 \rangle = \langle \psi_\mu | g; 1 \rangle \langle g; 1 | \hat{W} | e; 0 \rangle \quad (19)$$

Thus, the rate depends upon the cavity detuning.

$$\Gamma_{ex} = |\lambda_{eg}|^2 \frac{\Gamma_{cav}}{(\hbar\Gamma_{cav}/2)^2 + (\epsilon_e - \hbar\omega_{cav})^2}. \quad (20)$$

For strongly detuned cavities in which $|\epsilon_e - \hbar\omega_{cav}| \gg \hbar\Gamma_{cav}$, the exciton can not decay by radiating into the continuum. For a resonant cavity, on the other hand,

$$\Gamma_{ex, res} = \frac{\Omega_{Rabi}^2}{\Gamma_{cav}}. \quad (21)$$

However, this expression is not valid if the Rabi frequency is large compared to Γ_{cav} , which is the energy width over which the coupling between the exciton and the continuum is significant. That is to say, that the cavity lifetime must be significantly shorter than the Rabi oscillation period in order for Eq. 4 to be valid.

D. UP Decay

The probability amplitude that a continuum state $|\psi_\mu\rangle$ will be excited from the UP is proportional to the square of the following matrix element:

$$\begin{aligned} \langle \psi_\mu | \hat{W} | UP \rangle &= \frac{\hat{w}v + v' \sum_n v^2 / (E_\mu - E_n)}{(v^2 + (\hbar\Gamma_{cav}/2)^2 + E_\mu^2)^{1/2}} \\ &= \frac{\hat{w}v + v' E_\mu}{(v^2 + (\hbar\Gamma_{cav}/2)^2 + E_\mu^2)^{1/2}}. \end{aligned} \quad (22)$$

where we recall that \hat{w} is the phonon-mediated UP/LP coupling, and v and v' are the couplings between the LP and UP polaritons to the external photon states, respectively. The FGR expression is obtained by taking the trace over the vibrational degrees of freedom. and gives an expression of the form

$$\Gamma_U = \Gamma_{U, direct} + \Gamma_{U, seq} \quad (23)$$

The first term gives the direct rate resulting from the decay of the UP directly into the continuum via the v' coupling

$$\Gamma_{U, direct} = \frac{2\pi}{\hbar} \frac{(v')^2}{\delta} \frac{E_\mu^2}{v^2 + (\hbar\Gamma_{cav}/2)^2 + E_\mu^2} \quad (24)$$

which reduces to Eqs. 20 and 21 upon taking $\delta \rightarrow 0$ and setting $v' = v$. The second term arises from the fact that the UP can first decay to the LP, which in turn is also embedded in the continuum via the sequential pathway

$$|UP\rangle \xrightarrow{\hat{w}} |LP\rangle \xrightarrow{v} |k\rangle \quad (25)$$

If assume that the sequential path dominates so that the relaxation is sequential, the matrix element between UP and the continuum states factors into

$$\langle \psi_\mu | W | UP \rangle = \langle \psi_\mu | LP \rangle \langle LP | \hat{W} | UP \rangle = \langle \psi_\mu | LP \rangle \hat{w}. \quad (26)$$

This gives a FGR expression

$$\Gamma_{U,seq} = \langle \hat{w}^2 \rangle_{th} \frac{\Gamma_{cav}}{(\hbar\Gamma_{cav}/2)^2 + (\hbar\Omega_{Rabi})^2} \quad (27)$$

The matrix element $\langle \hat{w}^2 \rangle_{th}$ contains contribution from both the cavity and the internal vibronic coupling. If we average over a distribution of initial vibronic states

$$\langle \hat{w}^2 \rangle_{th} \approx g_{eg}^2 \langle \cos^2(2\eta) \rangle_{th} + \left(\frac{\hbar\omega S}{2} \right)^2 \langle \sin^2(2\eta) \rangle_{th} \quad (28)$$

For a resonant cavity, the mixing between the cavity and optical transition takes its maximum value with $\eta = \pi/4$. Furthermore, for a mixing angle of $\eta = \pi/4$, the contribution to G_{LU} from the internal non-adiabatic coupling is exactly equal to zero and is expected to be small compared to the reorganization energy $\hbar\omega S$. However, we can expand this about $X = 0$ at the crossing point, take the thermal average over the vibrational degrees of freedom, and use $2\lambda_{eg} = \hbar\Omega_{Rabi}$ to describe the coupling to between the cavity and the molecule. Expanding the mixing angle terms for small values of the nuclear displacement

$$\langle \hat{w}^2 \rangle_{th} \approx \left(\frac{\hbar\omega S}{2} \right)^2 \left(1 + \frac{(n_{th} + 1)(4g_{eg}^2 - (\hbar\omega S)^2)}{2(\hbar\Omega_{Rabi})^2} \right) + \dots \quad (29)$$

where we have summed over a thermal distribution of initial vibronic states and evaluated the density of states at the UP/LP energy gap.

The treatment is valid for sufficiently small coupling such that $\hbar\omega S/2$ is small compared to the cavity line-width $\hbar\Gamma_{cav}$. This means that the lifetime of the initial state UP is much longer than the lifetime for a cavity photon to decay into the continuum. This can be understood in terms of the period of a single Rabi oscillation between the two states, which is on the order of $(S\omega)^{-1}$, and the time-scale for the decay of the LP state into the continuum, which is Γ_{cav}^{-1} . If the LP state decays rapidly to the continuum, the system initially in UP will decay immediately to the continuum once it passes through the LP state and have a vanishingly small likelihood of returning to the UP at the end of the first Rabi oscillation. Consequently, the lower limit of the UP lifetime is set by the radiative decay of the cavity.

E. Decay of the relaxed LP state

We now consider the decay from the relaxed LP state shown in Fig. 2. In this scenario, we assume the LP can undergo vibronic relaxation from the Franck-Condon point to the lower energy geometry as depicted in Fig. 2. As the system moves away from the Franck-Condon point, the UP and LP states resolve back towards being purely cavity photon-like ($|g; 1\rangle$) and purely molecular exciton-like ($|e; 0\rangle$), respectively.

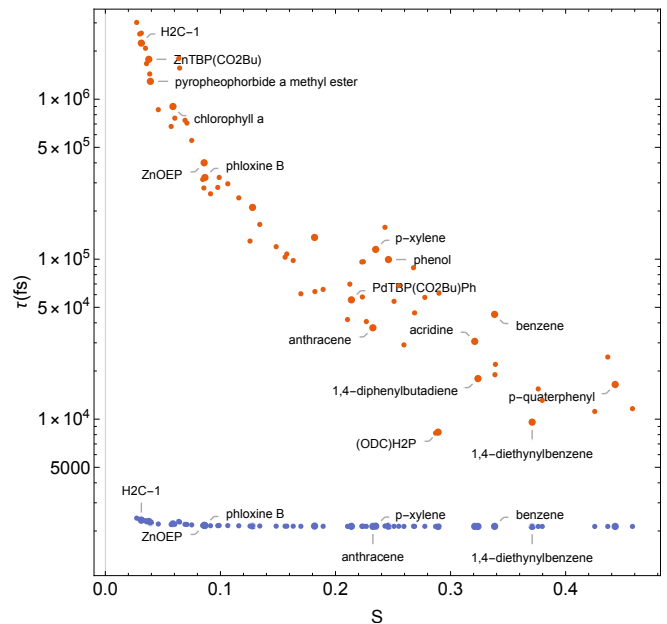


FIG. 3. Golden Rule estimates of UP (red) and LP (blue) lifetimes for various molecular systems based upon their Huang-Rhys factors, S and vibronic frequencies. Data for selected molecules are labeled on each plot and a complete data table including references and structures for each system is provided as Supplemental Material.

The analysis for the decay rate proceeds as above, except that the vibronic contribution is from the shifted state and that the density of states contribution is evaluated at the UP-LP gap *at the relaxed geometry*, i.e. $2\hbar\omega S$. Only if $2\hbar\omega S$ is small compared to the natural line-width of the cavity $\hbar\Gamma_{cav}$ will this state be able to decay into the continuum. Consequently, systems with large reorganization energies are more likely to form long-lived molecular excitons, held at their relaxed excited state geometries.

F. Molecular estimates

We can use the FGR expressions to provide estimates of the UP and LP lifetimes for a wide range of systems based upon their emission spectra. For organic conjugated systems, the vibronic fine structure is dominated by C=C stretching modes of from 150-200 meV with Huang-Rhys factors between 0.3 and 0.8. Table 1 in the Supplementary Information gives a summary of C=C frequencies and Huang-Rhys factors for various organic dye molecules and fluorophores obtained by analysing their fluorescence and absorption spectra taken from literature sources. For this we assume a model cavity with $\hbar\Omega_{Rabi} = 400$ meV corresponding to a Rabi oscillation period of $\tau_{Rabi} = 1.6$ fs. and a cavity photon lifetimes of 100 fs corresponding to $\hbar\Gamma_{cav} = 154$ meV which are typical in well-prepared molecular polariton systems. Gener-

ally, conjugated molecular systems have Huang-Rhys factors of $S \equiv 0.1 - 0.8$ and vibronic coupling is dominated by C=C stretching modes which are typically around $\hbar\omega = 200$ meV. Aside from the cavity couplings, all parameters for our model can be directly extracted from linear absorption/emission spectra of a molecular system.

We calculated reduced Huang-Rhys factors from spectral data freely available as part of the PhotochemCADTM program and database for a variety of organic chromophores. Out of the 339 compounds included in the PhotochemCADTM database, we identified a subset of compounds with 1) absorption and emission spectra available and 2) an identifiable vibronic structure. Using the peak position tool built into the PhotochemCADTM program, we determined the vibrational energy, $\hbar\omega$, from the energy difference between adjacent vibronic peaks.

Following the guidelines of de Jong *et al.*²⁹ for determining S from experimental spectra, we then converted each spectrum to an energy scale. Next we converted the absorbance and emission to transition moment squared, $W(E)$, using the relations $A(E) \propto EW(E)$ and $\phi(E) \propto E^3W(E)$, where $A(E)$ is the absorbance and $\phi(E)$ is the photon flux per unit of energy. We then calculated the barycenter of the baseline-corrected absorbance and emission spectra by evaluating

$$E_{bc} = \frac{\int W(E)E dE}{\int W(E) dE} \quad (30)$$

using Simpson’s rule for each spectrum. Finally, for each compound we calculated the reduced Huang-Rhys parameter with the relation $\Delta E_{bc} = 2S$, where ΔE_{bc} is the difference between the barycenters of the absorption and emission spectra. A complete list of the couplings and sources is given in the SI. From this data, we report estimated UP and LP decay times for a variety of common compounds in Fig. 3(a,b).

Fig 3(a), the model predicts a broad range of UP lifetimes ranging from 100ps to less than 500 fs, largely determined by the variation in Huang-Rhys factors. Small Huang-Rhys factors imply very weak vibronic coupling and small distortion of the molecule in its excited electronic state. Consequently, the system remains in the UP state near the avoided crossing region for long time. The LP lifetime spans a much narrower range than the UP lifetime. It is also surprisingly predicted to be shorter than the UP lifetime. This lifetime is entirely dominated by the fact that the relaxed LP is almost entirely excitonic-like ($|e;0\rangle$) rather than photon-like ($|g;1\rangle$). Consequently, relaxation from this state via cavity emission is an activated process with $2\hbar\omega S \approx \hbar\Omega_{Rabi}$.

III. DISCUSSION

The polariton lifetime dictates any eventual “polariton chemistry” that might be induced or manipulated

via coupling to the cavity. Here, we consider the the lifetime for polaritons in resonant cavities, where we anticipate the strongest coupling between the molecular and photon degrees of freedom. The long-lifetimes of these states predicted by our model is directly related to the fact that we prepare the system in a light-matter eigenstate. We also assume that the cavities themselves are of sufficiently high-quality that strong-coupling can be achieved in the sense that Rabi splitting between UP and LP branches is larger than the emission linewidths of the polaritons. These are reasonable assumptions that are consistent with contemporary experimental conditions.

ACKNOWLEDGMENTS

The work at the University of Houston was funded in part by the National Science Foundation (CHE-1664971, CHE-1836080, DMR-1903785) and the Robert A. Welch Foundation (E-1337). GO acknowledges the support of the University of Houston Honors College for a Summer Undergraduate Research (SURF) fellowship. The work at Georgia Tech was funded by the National Science Foundation (DMR-1904293).

DATA AVAILABILITY

The data that support the findings of this study are available from the corresponding author upon reasonable request.

- ¹E. Eizner, L. A. Martínez-Martínez, J. Yuen-Shou, and S. Kéna-Cohen, “Inverting singlet and triplet excited states using strong light–matter coupling,” Arxiv **1903.09251v1**, 1 (2016).
- ²J. Feist, J. Galego, and F. J. Garcia-Vidal, “Polaritonic chemistry with organic molecules,” ACS Photonics **5**, 205 (2018).
- ³J. Flick, M. Ruggenthaler, H. Appel, and A. Rubio, “Atoms and molecules in cavities: From weak to strong coupling in qcd chemistry,” Proc. Natl. Acad. Sci. U. S. A. **114**, 3026 (2017).
- ⁴J. Galego, F. J. Garcia-Vidal, and J. Feist, “Cavity-induced modifications of molecular structure in the strong-coupling regime,” Phys. Rev. X **5**, 041022 (2015).
- ⁵J. Galego, F. J. Garcia-Vidal, and J. Feist, “Suppressing photochemical reactions with quantized light fields,” Nat. Commun. **7**, 13841 (2016).
- ⁶J. Galego, F. J. Garcia-Vidal, and J. Feist, “Many-molecule reaction triggered by a single photon in polaritonic chemistry,” Phys. Rev. Lett. **119**, 136001 (2017).
- ⁷V. M. Agranovich, M. Litinskaia, and D. G. Lidzey, “Cavity polaritons in microcavities containing disordered organic semiconductors,” Phys. Rev. B: Condens. Matter Mater. Phys. **67**, 085311 (2003).
- ⁸F. Herrera and F. C. Spano, “Cavity-controlled chemistry in molecular ensembles,” Phys. Rev. Lett. **116**, 238301 (2016).
- ⁹F. Herrera and F. C. Spano, “Dark vibronic polaritons and the spectroscopy of organic microcavities,” Phys. Rev. Lett. **118**, 223601 (2017).
- ¹⁰F. Herrera and F. C. Spano, “Absorption and photoluminescence in organic cavity qcd,” Phys. Rev. A: At., Mol., Opt. Phys. **95**, 053867 (2017).
- ¹¹F. Herrera and F. C. Spano, “Theory of nanoscale organic cavities: The essential role of vibration-photon dressed states,” ACS Photonics **5**, 65 (2018).

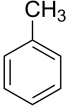
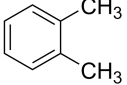
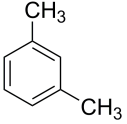
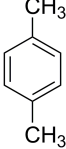
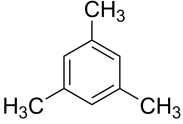
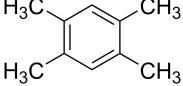
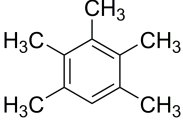
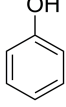
- ¹²C. Cohen-Tannoudji, J. Dupont-Roc, and G. Grynberg, *Atom-photon Interactions* (Wiley-Interscience, 1992).
- ¹³J. Mony, M. Hertzog, K. Kushwaha, and K. Börjesson, "Angle-independent polariton emission lifetime shown by perylene hybridized to the vacuum field inside a fabry-pérot cavity," *The Journal of Physical Chemistry C* **122**, 24917–24923 (2018).
- ¹⁴S. Wang, T. Chervy, J. George, J. A. Hutchison, C. Genet, and T. W. Ebbesen, "Quantum yield of polariton emission from hybrid light-matter states," *The Journal of Physical Chemistry Letters* **5**, 1433–1439 (2014).
- ¹⁵D. Ballarini, M. De Giorgi, S. Gambino, G. Lerario, M. Mazzeo, A. Genco, G. Accorsi, C. Giansante, S. Colella, S. D'Agostino, P. Cazzato, D. Sanvitto, and G. Gigli, "Polariton-induced enhanced emission from an organic dye under the strong coupling regime," *Advanced Optical Materials* **2**, 1076–1081 (2014), <https://onlinelibrary.wiley.com/doi/pdf/10.1002/adom.201400226>.
- ¹⁶D. G. Lidzey, A. M. Fox, M. D. Rahn, M. S. Skolnick, V. M. Agranovich, and S. Walker, "Experimental study of light emission from strongly coupled organic semiconductor microcavities following nonresonant laser excitation," *Phys. Rev. B* **65**, 195312 (2002).
- ¹⁷F. Thouin, A. R. Srimath Kandada, D. A. Valverde-Chávez, D. Cortecchia, I. Bargigia, A. Petrozza, X. Yang, E. R. Bittner, and C. Silva, "Electron-phonon couplings inherent in polarons drive exciton dynamics in two-dimensional metal-halide perovskites," *Chem. Mater.* **31**, 7085–7091 (2019).
- ¹⁸X. Yang and E. R. Bittner, "Intramolecular charge-and energy-transfer rates with reduced modes: Comparison to marcus theory for donor-bridge-acceptor systems," *J. Phys. Chem. A* **118**, 5196–5203 (2014).
- ¹⁹X. Yang and E. R. Bittner, "Computing intramolecular charge and energy transfer rates using optimal modes," *J. Chem. Phys.* **142**, 244114 (2015).
- ²⁰X. Yang, T. Keane, M. Delor, A. J. Meijer, J. Weinstein, and E. R. Bittner, "Identifying electron transfer coordinates in donor-bridge-acceptor systems using mode projection analysis," *Nat. Commun.* **8**, 14554 (2017).
- ²¹X. Yang, A. Pereverzev, and E. R. Bittner, "Inelastic charge-transfer dynamics in donor-bridge-acceptor systems using optimal modes," *Adv. Chem. Phys.* **163**, 167–194 (2018).
- ²²S. Karabunarliev and E. R. Bittner, "Dissipative dynamics of spin-dependent electron-hole capture in conjugated polymers," *J. Chem. Phys.* **119**, 3988–3995 (2003).
- ²³S. Karabunarliev and E. R. Bittner, "Polaron-excitons and electron-vibrational band shapes in conjugated polymers," *J. Chem. Phys.* **118**, 4291–4296 (2003).
- ²⁴S. Karabunarliev, E. R. Bittner, and M. Baumgarten, "Franck-Condon spectra and electron-libration coupling in parapolymers," *J. Chem. Phys.* **114**, 5863–5870 (2001).
- ²⁵S. Karabunarliev and E. R. Bittner, "Electroluminescence yield in donor-acceptor copolymers and diblock polymers: A comparative theoretical study," *J. Phys. Chem. B* **108**, 10219–10225 (2004).
- ²⁶S. Karabunarliev and E. R. Bittner, "Spin-dependent electron-hole capture kinetics in luminescent conjugated polymers," *Phys. Rev. Lett.* **90**, 057402 (2003).
- ²⁷S. Karabunarliev and E. R. Bittner, "Publisher's note: Spin-dependent electron-hole capture kinetics in luminescent conjugated polymers [phys. rev. lett., 057402 (2003)]," *Phys. Rev. Lett.* **90**, 079901 (2003).
- ²⁸M. Tavis and F. W. Cummings, "Approximate solutions for an n-molecule radiation-field hamiltonian," *Phys. Rev.* **188**, 692 (1969).
- ²⁹M. de Jong, L. Seijo, A. Meijerink, and F. T. Rabouw, "Resolving the ambiguity in the relation between stokes shift and huang-rhys parameter," *Phys. Chem. Chem. Phys.* **17**, 16959–16969 (2015).
- ³⁰I. B. Berlman, *Handbook of fluorescence spectra of aromatic molecules*, 2nd ed. (Academic Press, New York, 1971).
- ³¹W. R. Dawson and M. W. Windsor, "Fluorescence yields of aromatic compounds," *J. Phys. Chem.* **72**, 3251–3260 (1968).
- ³²C. Santiago, R. W. Gandour, K. Houk, W. Nutakul, W. E. Cravey, and R. P. Thummel, "Photoelectron and ultraviolet spectra of small-ring fused aromatic molecules as probes of aromatic ring distortions," *J. Am. Chem. Soc.* **100**, 3730–3737 (1978).
- ³³P. M. Froehlich and H. A. Morrison, "Alkylbenzene luminescence," *J. Phys. Chem.* **76**, 3566–3570 (1972).
- ³⁴Y. Nakayama, Y. Ichikawa, and T. Matsuo, "A study of the charge-transfer complexes. i. the interaction of pyromellitic dianhydride with polymethylbenzenes," *Bull. Chem. Soc. Jpn.* **38**, 1674–1683 (1965).
- ³⁵G. Grabner, G. Koehler, G. Marconi, S. Monti, and E. Venuti, "Photophysical properties of methylated phenols in nonpolar solvents," *J. Phys. Chem.* **94**, 3609–3613 (1990).
- ³⁶C. A. van Walree, M. R. Roest, W. Schuddeboom, L. W. Jenneskens, J. W. Verhoeven, J. M. Warman, H. Kooijman, and A. L. Spek, "Comparison between sime2 and cme2 spacers as σ -bridges for photoinduced charge transfer," *J. Am. Chem. Soc.* **118**, 8395–8407 (1996).
- ³⁷M. Yamakawa, T. Kubota, H. Akazawa, and I. Tanaka, "Electronic spectra and electronic structures of benzonitrile n-oxide and its derivatives," *Bull. Chem. Soc. Jpn.* **41**, 1046–1055 (1968).
- ³⁸N. Bayliss and L. Hulme, "Solvent effects in the spectra of benzene, toluene, and chlorobenzene at 2600 and 2000 \AA ," *Aus. J. Chem.* **6**, 257–277 (1953).
- ³⁹A. Harriman and B. W. Rockett, "Comparative study of spin-orbital coupling for halogenated ethylbenzenes by a study of their fluorescence," *J. Chem. Soc. Perkin Trans.* , 217–219 (1974).
- ⁴⁰A. Pelter and D. E. Jones, "The preparation and some properties of substituted phenylene-ethynylene and phenylenebuta-1,3-diyne polymers," *J. Chem. Soc. Perkin Trans.* , 2289–2294 (2000).
- ⁴¹F. Marchioni, A. Juris, M. Lobert, U. P. Seelbach, B. Kahlert, and F.-G. Klärner, "Luminescent host-guest complexes involving molecular clips and tweezers and tetracyanobenzene," *New J. Chem.* **29**, 780–784 (2005).
- ⁴²A. M. Müller, Y. S. Avlasevich, K. Müllen, and C. J. Bardeen, "Evidence for exciton fission and fusion in a covalently linked tetracene dimer," *Chem. Phys. Lett.* **421**, 518–522 (2006).
- ⁴³W. H. Flora, H. K. Hall, and N. R. Armstrong, "Guest emission processes in doped organic light-emitting diodes: Use of phthalocyanine and naphthalocyanine near-ir dopants," *J. Phys. Chem. B* **107**, 1142–1150 (2003).
- ⁴⁴I. Chvátal, J. Vymětal, J. Pecha, V. Šimánek, L. Dolejš, J. Bartoň, and J. Fryčka, "Isolation and identification of by-products of gas phase catalytic oxidation of anthracene to 9,10-anthraquinone," *Coll. Czech. Chem. Commun.* **48**, 112–122 (1983).
- ⁴⁵T. Barros, I. Cuccovia, J. Farah, J. Masini, H. Chaimovich, and M. Politi, "Mechanism of 1, 4, 5, 8-naphthalene tetracarboxylic acid dianhydride hydrolysis and formation in aqueous solution," *Org. Biomol. Chem.* **4**, 71–82 (2006).
- ⁴⁶G. Drefahl and G. Plötner, "Untersuchungen über stilbene, xx. polyphenyl-polybutadiene," *Chem. Ber.* **91**, 1285–1289 (1958).
- ⁴⁷S. Chattopadhyay, P. Das, and G. Hug, "Photoprocesses in diphenylpolyenes. oxygen and heavy-atom enhancement of triplet yields," *J. Am. Chem. Soc.* **104**, 4507–4514 (1982).
- ⁴⁸R. F. Chen, "Measurements of absolute values in biochemical fluorescence spectroscopy," *J. Res. Nat. Bur. Stand. Sect. A* **76**, 593–606 (1972).
- ⁴⁹G. D. Fasman, *Practical handbook of biochemistry and molecular biology* (CRC press, 1989).
- ⁵⁰J. J. Aaron, M. Maafi, C. Párkányi, and C. Boniface, "Quantitative treatment of the solvent effects on the electronic absorption and fluorescence spectra of acridines and phenazines. the ground and first excited singlet-state dipole moments," *Spectrochim. Acta A* **51**, 603–615 (1995).

- ⁵¹L. A. Diverdi and M. R. Topp, "Subnanosecond time-resolved fluorescence of acridine in solution," *J. Phys. Chem.* **88**, 3447–3451 (1984).
- ⁵²R. Hegde, P. Thimmaiah, M. C. Yerigeri, G. Krishnegowda, K. N. Thimmaiah, and P. J. Houghton, "Anti-calmodulin acridone derivatives modulate vinblastine resistance in multidrug resistant (mdr) cancer cells," *Eur. J. Med. Chem.* **39**, 161–177 (2004).
- ⁵³S. Rentsch, R. Danielius, and R. Gadonas, "Bestimmung von lebensdauern und transientenabsorptionsspektren von polymethinfarbstoffen aus pikosekundenspektroskopischen messungen," *J. Signalaufz-Mater.* **12**, 319–328 (1984).
- ⁵⁴D. N. Dempster, T. Morrow, R. Rankin, and G. Thompson, "Photochemical characteristics of the mode-locking dyes 1, 1'-diethyl-4, 4'-carbocyanine iodide (cryptocyanine, dci) and 1, 1'-diethyl-2, 2'-dicarb," *Chem. Phys. Lett.* **18**, 488–492 (1973).
- ⁵⁵P. J. Sims, A. S. Waggoner, C.-H. Wang, and J. F. Hoffman, "Mechanism by which cyanine dyes measure membrane potential in red blood cells and phosphatidylcholine vesicles," *Biochem.* **13**, 3315–3330 (1974).
- ⁵⁶A. Waggoner, R. De Biasio, P. Conrad, G. Bright, L. Ernst, K. Ryan, M. Nederlof, and D. Taylor, "Multiple spectral parameter imaging," *Methods in cell biology* **30**, 449–478 (1989).
- ⁵⁷K.-y. Tomizaki, R. S. Loewe, C. Kirmaier, J. K. Schwartz, J. L. Retsek, D. F. Bocian, D. Holten, and J. S. Lindsey, "Synthesis and photophysical properties of light-harvesting arrays comprised of a porphyrin bearing multiple perylene-monoimide accessory pigments," *J. Org. Chem.* **67**, 6519–6534 (2002).
- ⁵⁸A. Rademacher, S. Märkle, and H. Langhals, "Loesliche perylenfluoreszenzfarbstoffe mit hoher photostabilitaet," *Chem. Ber.* , 2927–2934 (1982).
- ⁵⁹S. Prathapan, S. I. Yang, J. Seth, M. A. Miller, D. F. Bocian, D. Holten, and J. S. Lindsey, "Synthesis and excited-state photodynamics of perylene-porphyrin dyads. I. parallel energy and charge transfer via a diphenylethyne linker," *J. Phys. Chem. B* **105**, 8237–8248 (2001).
- ⁶⁰S. H. Lee, D. H. Nam, and C. B. Park, "Screening xanthene dyes for visible light-driven nicotinamide adenine dinucleotide regeneration and photoenzymatic synthesis," *Adv. Synth. Catal.* **351**, 2589–2594 (2009).
- ⁶¹P. G. Seybold, M. Gouterman, and J. Callis, "Calorimetric, photometric and lifetime determinations of fluorescence yields of fluorescein dyes," *Photochem. Photobiol.* **9**, 229–242 (1969).
- ⁶²P. Myslinski and D. Wiczorek, "Differential anisotropy of polarizability measured by picosecond transient dichroism and birefringence," *J. Chem. Phys.* **92**, 969–977 (1990).
- ⁶³O. Galangau, C. Dumas-Verdes, R. Méallet-Renault, and G. Clavier, "Rational design of visible and nir distyryl-bodipy dyes from a novel fluorinated platform," *Org. Biomol. Chem.* **8**, 4546–4553 (2010).
- ⁶⁴E. Zass, H. P. Isenring, R. Etter, and A. Eschenmoser, "Der einbau von magnesium in liganden der chlorophyll-reihe mit (2, 6-di-*t*-butyl-4-methylphenoxy) magnesiumjodid," *Helv. Chim. Acta* **63**, 1048–1067 (1980).
- ⁶⁵O. Ohno, Y. Kaizu, and H. Kobayashi, "Luminescence of some metalloporphins including the complexes of the iib metal group," *J. Chem. Phys.* **82**, 1779–1787 (1985).
- ⁶⁶J. W. Buchler and L. Puppe, "Metallkomplexe mit tetrapyrrol-liganden, iil) metallchelat des α . γ -dimethyl- α . γ -dihydro-octaäthylporphins durch reduzierende methylierung von octaäthylporphinato-zink," *Liebigs Ann. Chem.* **740**, 142–163 (1970).
- ⁶⁷A. Ghosh, S. M. Mobin, R. Fröhlich, R. J. Butcher, D. K. Maity, and M. Ravikanth, "Effect of five membered versus six membered meso-substituents on structure and electronic properties of mg (ii) porphyrins: A combined experimental and theoretical study," *Inorg. Chem.* **49**, 8287–8297 (2010).
- ⁶⁸J.-P. Strachan, D. F. O'Shea, T. Balasubramanian, and J. S. Lindsey, "Rational synthesis of meso-substituted chlorin building blocks," *J. Org. Chem.* **65**, 3160–3172 (2000).
- ⁶⁹G. H. Barnett, M. F. Hudson, and K. M. Smith, "Concerning meso-tetraphenylporphyrin purification," *J. Chem. Soc. Perkin Trans.* , 1401–1403 (1975).
- ⁷⁰S. I. Yang, J. Seth, J.-P. STRACHAN, S. Gentemann, D. Kim, D. Holten, J. S. Lindsey, and D. F. Bocian, "Ground and excited state electronic properties of halogenated tetraarylporphyrins. tuning the building blocks for porphyrin-based photonic devices," *J. Porphyrins Phthalocyanines* **3**, 117–147 (1999).
- ⁷¹J. S. Lindsey and J. N. Woodford, "A simple method for preparing magnesium porphyrins," *Inorg. Chem.* **34**, 1063–1069 (1995).
- ⁷²J. B. Kim, J. J. Leonard, and F. R. Longo, "Mechanistic study of the synthesis and spectral properties of meso-tetraarylporphyrins," *J. Am. Chem. Soc.* **94**, 3986–3992 (1972).
- ⁷³J. Grancho, M. Pereira, M. d. G. Miguel, A. R. Gonsalves, and H. Burrows, "Synthesis, spectra and photophysics of some free base tetrafluoroalkyl and tetrafluoroaryl porphyrins with potential applications in imaging," *Photochem. Photobiol.* **75**, 249–256 (2002).
- ⁷⁴A. Gradyushko, A. Sevchenko, K. Solovyov, and M. Tsvirko, "Energetics of photophysical processes in chlorophyll-like molecules," *Photochem. Photobiol.* **11**, 387–400 (1970).
- ⁷⁵D. Berezin, O. Toldina, and E. Kudrik, "Complex formation and spectral properties of meso-phenyltetraenzoporphyrins in pyridine and *n*, *n*-dimethylformamide," *Russ. J. Gen. Chem.* **73**, 1309–1314 (2003).
- ⁷⁶O. S. Finikova, A. V. Cheprakov, and S. A. Vinogradov, "Synthesis and luminescence of soluble meso-unsubstituted tetrabenzoz- and tetranaphtho [2, 3] porphyrins," *J. Org. Chem.* **70**, 9562–9572 (2005).
- ⁷⁷O. S. Finikova, A. V. Cheprakov, I. P. Beletskaya, P. J. Carroll, and S. A. Vinogradov, "Novel versatile synthesis of substituted tetrabenzoporphyrins," *J. Org. Chem.* **69**, 522–535 (2004).
- ⁷⁸J. M. Dixon, M. Taniguchi, and J. S. Lindsey, "Photochemcad 2: a refined program with accompanying spectral databases for photochemical calculations," *Photochem. Photobiol.* **81**, 212–213 (2005).
- ⁷⁹Z. Gross, N. Galili, and I. Saltsman, "The first direct synthesis of corroles from pyrrole," *Angew. Chem. Int. Ed.* **38**, 1427–1429 (1999).
- ⁸⁰P. G. Seybold and M. Gouterman, "Porphyrins: Xiii: Fluorescence spectra and quantum yields," *J. Mol. Spectrosc.* **31**, 1–13 (1969).
- ⁸¹M. Whalley, "Conjugated macrocycles. part xxxii. absorption spectra of tetrazaporphins and phthalocyanines. formation of pyridine salts," *J. Chem. Soc.* , 866–869 (1961).
- ⁸²D. S. Lawrence and D. G. Whitten, "Photochemistry and photophysical properties of novel, unsymmetrically substituted metallophthalocyanines," *Photochem. Photobiol.* **64**, 923–935 (1996).
- ⁸³H. H. Strain, M. R. Thomas, and J. J. Katz, "Spectral absorption properties of ordinary and fully deuteriated chlorophylls a and b," *Biochim. Biophys. Acta* **75**, 306–311 (1963).
- ⁸⁴G. Weber and F. Teale, "Determination of the absolute quantum yield of fluorescent solutions," *Trans. Faraday Soc.* **53**, 646–655 (1957).
- ⁸⁵P. H. Hynninen and S. Lötjönen, "Large-scale preparation of crystalline (10s)-chlorophylls a and b," *Synthesis* **9**, 705–708 (1983).
- ⁸⁶I. Eichwurz, H. Stiel, and B. Röder, "Photophysical studies of the pheophorbide a dimer," *J. Photochem. Photobiol. B* **54**, 194–200 (2000).
- ⁸⁷G. Zheng, H. Li, M. Zhang, S. Lund-Katz, B. Chance, and J. D. Glickson, "Low-density lipoprotein reconstituted by pyropheorbide cholesteryl oleate as target-specific photosensitizer," *Bioconjugate Chem.* **13**, 392–396 (2002).
- ⁸⁸S. Al-Omari and A. Ali, "Photodynamic activity of pyropheorbide methyl ester and pyropheorbide a in dimethylformamide solution," *Gen. Physiol. Biophys* **28**, 70–77 (2009).
- ⁸⁹K. M. Smith, D. A. Goff, and D. J. Simpson, "The meso substitution of chlorophyll derivatives: direct route for transformation of

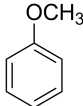
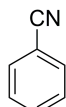
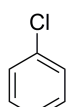
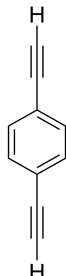
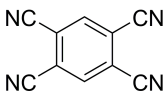
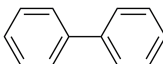
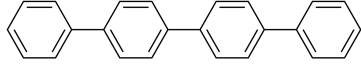
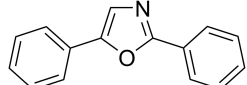
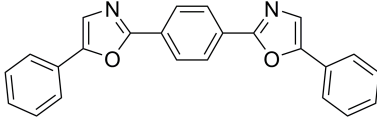
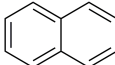
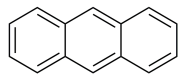
- bacteriopheophorbides d into bacteriopheophorbides c." J. Am. Chem. Soc. **107**, 4946–4954 (1985).
- ⁹⁰S.-i. Sasaki, K. Mizutani, M. Kunieda, and H. Tamiaki, "Synthesis, modification, and optical properties of c3-ethynylated chlorophyll derivatives," Tetrahedron Lett. **49**, 4113–4115 (2008).
- ⁹¹E. S. Nyman and P. H. Hynninen, "Research advances in the use of tetrapyrrolic photosensitizers for photodynamic therapy," J. Photochem. Photobiol. B **73**, 1–28 (2004).
- ⁹²A. Kay, R. Humphry-Baker, and M. Graetzel, "Artificial photosynthesis. 2. investigations on the mechanism of photosensitization of nanocrystalline tio₂ solar cells by chlorophyll derivatives," J. Phys. Chem. **98**, 952–959 (1994).
- ⁹³E. Zenkevich, E. Sagun, V. Knyukshto, A. Shulga, A. Mironov, O. Efremova, R. Bonnett, S. P. Songca, and M. Kassem, "Photophysical and photochemical properties of potential porphyrin and chlorin photosensitizers for pdt," J. Photochem. Photobiol. B **33**, 171–180 (1996).
- ⁹⁴J. K. Hooper, T. W. Sery, and N. Yamamoto, "Photodynamic sensitizers from chlorophyll: Purpurin-18 and chlorin *p6*," Photochem. Photobiol. **48**, 579–582 (1988).
- ⁹⁵H. W. J. Whitlock, R. Hanauer, M. Y. Oester, and B. K. Bower, "Diimide reduction of porphyrins," J. Am. Chem. Soc. **91**, 7485–7489 (1969).
- ⁹⁶K. Aravindu, H.-J. Kim, M. Taniguchi, P. L. Dilbeck, J. R. Diers, D. F. Bocian, D. Holten, and J. S. Lindsey, "Synthesis and photophysical properties of chlorins bearing 0–4 distinct meso-substituents," Photochem. Photobiol. Sci. **12**, 2089–2109 (2013).
- ⁹⁷J.-P. Strachan, S. Gentemann, J. Seth, W. A. Kalsbeck, J. S. Lindsey, D. Holten, and D. F. Bocian, "Effects of orbital ordering on electronic communication in multiporphyrin arrays," J. Am. Chem. Soc. **119**, 11191–11201 (1997).
- ⁹⁸M. Taniguchi, H.-J. Kim, D. Ra, J. K. Schwartz, C. Kirmaier, E. Hindin, J. R. Diers, S. Prathapan, D. F. Bocian, D. Holten, *et al.*, "Synthesis and electronic properties of regioisomerically pure oxochlorins," J. Org. Chem. **67**, 7329–7342 (2002).

SUPPLEMENTARY INFORMATION

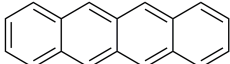
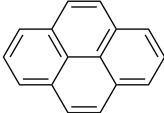
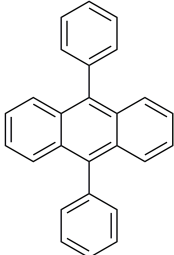
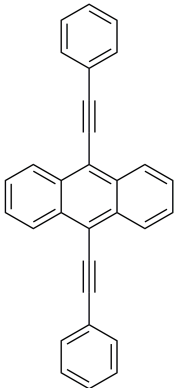
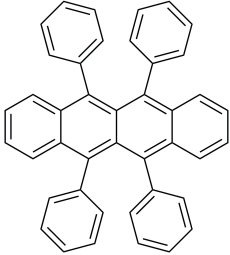
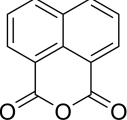
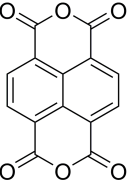
IV. DATA TABLE

Compound	$\hbar\omega$ (eV)	S (reduced)	τ_{LP} (ps)	τ_{UP} (ps)	References
 benzene	0.11	0.34	2.1	45	30, 31
 toluene	0.12	0.44	2.1	24	30
 o-xylene	0.14	0.27	2.1	46	32, 33
 m-xylene	0.14	0.25	2.1	55	30, 33
 p-xylene	0.10	0.23	2.1	115	30, 33
 mesitylene	0.12	0.25	2.1	68	33, 34
 durene	0.15	0.22	2.1	58	33, 34
 pentamethylbenzene	0.08	0.24	2.1	158	33, 34
 phenol	0.10	0.25	2.1	99	30, 35

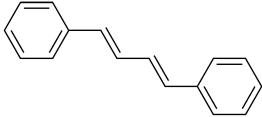
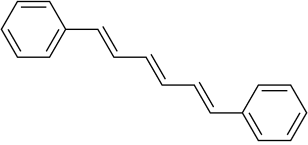
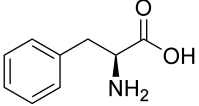
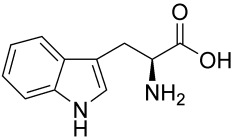
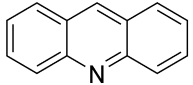
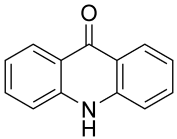
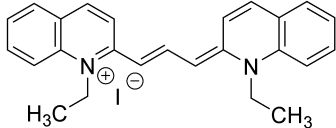
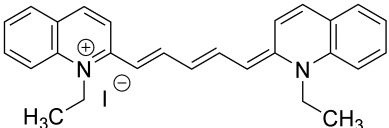
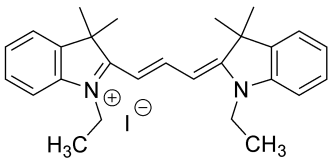
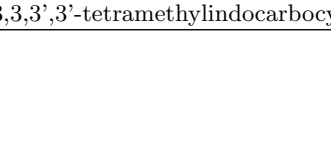
Continued on next page

Compound	$\hbar\omega$ (eV)	S (reduced)	τ_{LP} (ps)	τ_{UP} (ps)	References
 anisole	0.12	0.22	2.1	96	36
 benzonitrile	0.12	0.22	2.1	96	36, 37
 chlorobenzene	0.12	0.28	2.1	58	38, 39
 1,4-diethynylbenzene	0.23	0.37	2.1	9.5	40
 1,2,4,5-tetracyanobenzene	0.15	0.16	2.1	107	41
 biphenyl	0.16	0.61	2.1	7.3	30
 p-terphenyl	0.16	0.46	2.1	11.6	30
 p-quaterphenyl	0.14	0.44	2.1	16.5	30
 2,5-diphenyloxazole [PPO]	0.19	0.38	2.1	13.0	30
 1,4-Bis(5-phenyl-2-oxazolyl)benzene, [POPOP]	0.18	0.26	2.1	29.1	30
 naphthalene	0.17	0.38	2.1	15454	30
					

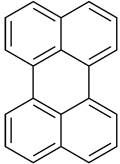
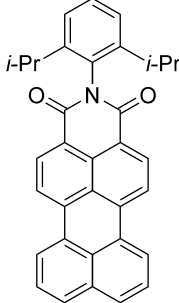
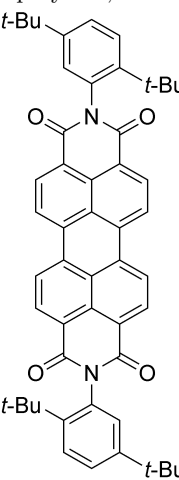
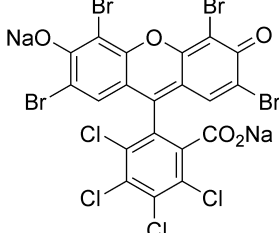
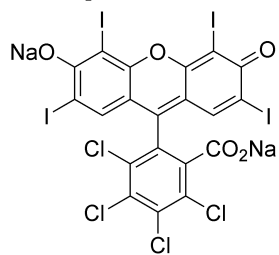
Continued on next page

Compound	$\hbar\omega$ (eV)	S (reduced)	τ_{LP} (ps)	τ_{UP} (ps)	References
anthracene 	0.18	0.23	2.1	37.2	30
tetracene 	0.18	0.18	2.1	62.7	30, 42
pyrene 	0.17	0.34	2.1	19.0	30
9,10-diphenylanthracene 	0.18	0.23	2.1	40.7	30
9,10-Bis(phenylethynyl)anthracene 	0.12	0.18	2.1	136	30
rubrene 	0.17	0.19	2.1	64.7	30, 43
1,8-naphthalic anhydride 	0.11	0.29	2.1	61.3	44

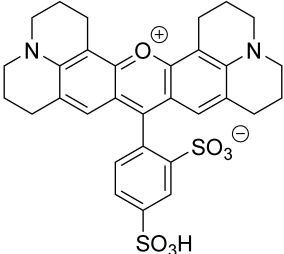
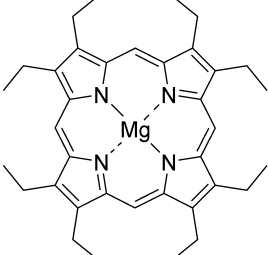
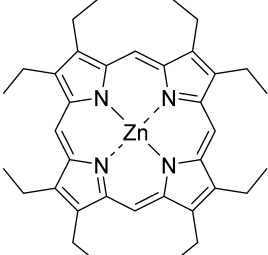
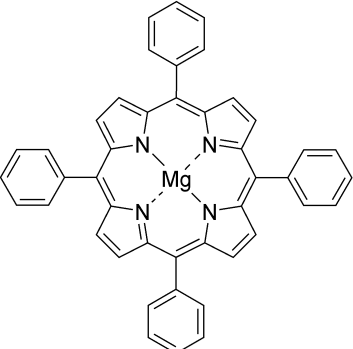
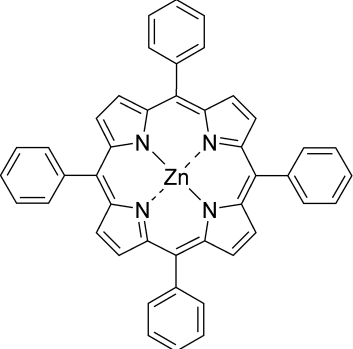
Continued on next page

Compound	$\hbar\omega$ (eV)	S (reduced)	τ_{LP} (ps)	τ_{UP} (ps)	References
1,4,5,8-naphthalenetetracarboxylic dianhydride 	0.19	0.21	2.1	42.0	45
1,4-diphenylbutadiene 	0.19	0.32	2.1	17.9	46, 47
1,6-diphenylhexatriene 	0.18	0.43	2.1	11.2	47
L-phenylalanine 	0.10	0.27	2.1	88.4	48, 49
L-tryptophan 	0.15	0.58	2.1	9.31	48, 49
acridine 	0.14	0.32	2.1	30.6	50, 51
acridone 	0.16	0.34	2.1	22.0	31, 52
1,1'-diethyl-2,2'-carbocyanine iodide 	0.15	0.10	2.2	280	53
1,1'-diethyl-2,2'-dicarbocyanine iodide 	0.15	0.06	2.2	761	54
1,1'-diethyl-3,3,3',3'-tetramethylindocarbocyanine iodide 	0.14	0.13	2.1	211	55, 56

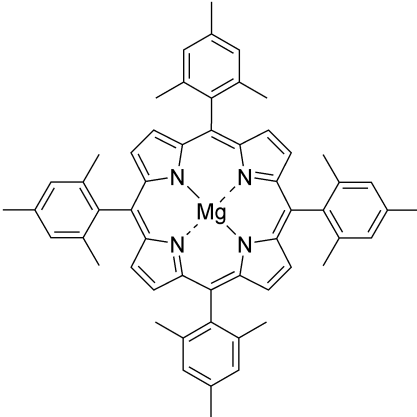
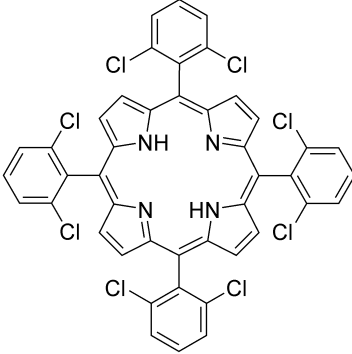
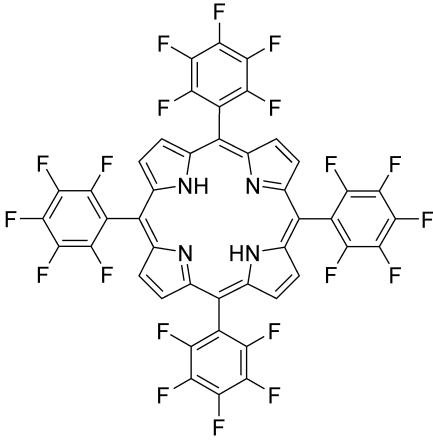
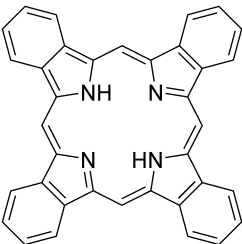
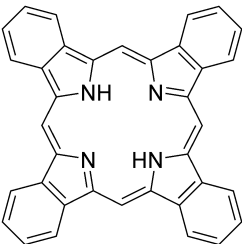
Continued on next page

Compound	$\hbar\omega$ (eV)	S (reduced)	τ_{LP} (ps)	τ_{UP} (ps)	References
 <p>perylene</p>	0.19	0.17	2.1	61.0	30
 <p>perylene, PMI</p>	0.14	0.21	2.1	70.0	57
 <p>perylene, PDI</p>	0.18	0.13	2.1	130	58, 59
 <p>phloxine B</p>	0.16	0.09	2.2	324	60
 <p>rose bengal</p>	0.17	0.08	2.2	315	61

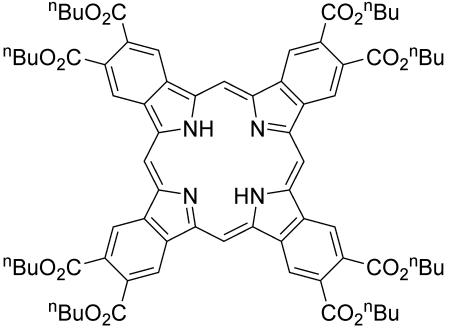
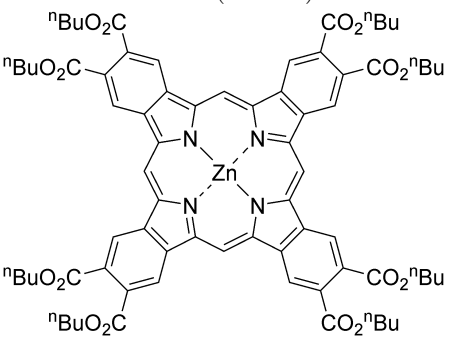
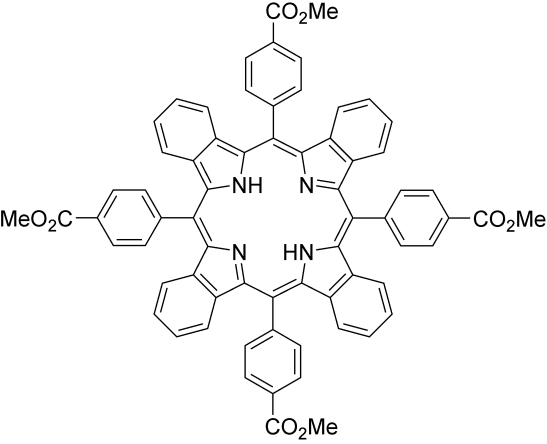
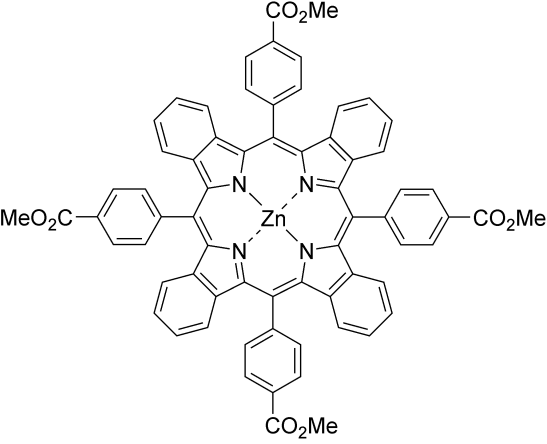
Continued on next page

Compound	$\hbar\omega$ (eV)	S (reduced)	τ_{LP} (ps)	τ_{UP} (ps)	References
 sulforhodamine 101	0.14	0.08	2.2	552	62, 63
 MgOEP	0.14	0.10	2.2	324	64
 ZnOEP	0.15	0.09	2.2	401	65, 66
 MgTPP	0.14	0.12	2.2	242	67, 68
 ZnTPP					

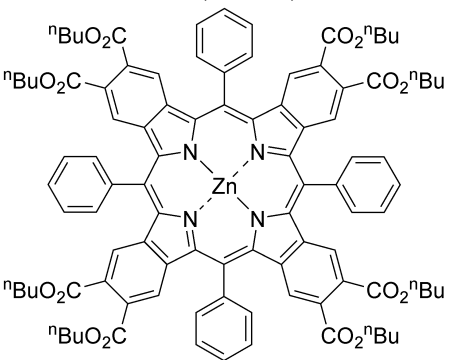
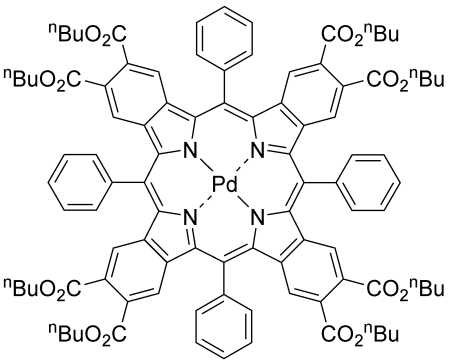
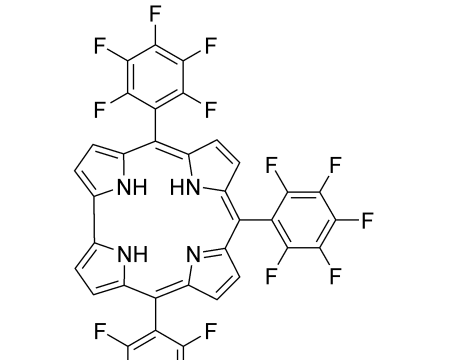
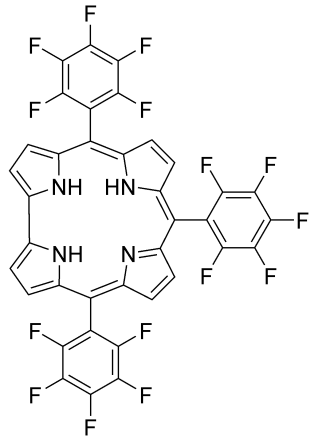
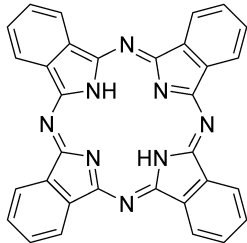
Continued on next page

Compound	$\hbar\omega$ (eV)	S (reduced)	τ_{LP} (ps)	τ_{UP} (ps)	References
ZnTPP 	0.16	0.15	2.1	120	69, 68
MgTMP 	0.15	0.13	2.1	165	70, 71
(ODC)H2P 	0.31	0.29	2.1	8.29	72, 70
C6F5-H2P 	0.32	0.29	2.1	8.18	73
tetrabenzoporphine 	0.17	0.09	2.2	256	74, 75

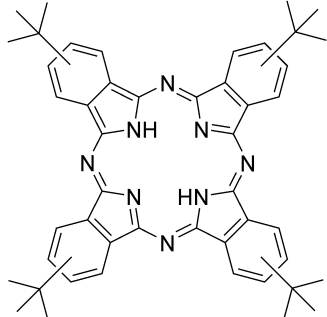
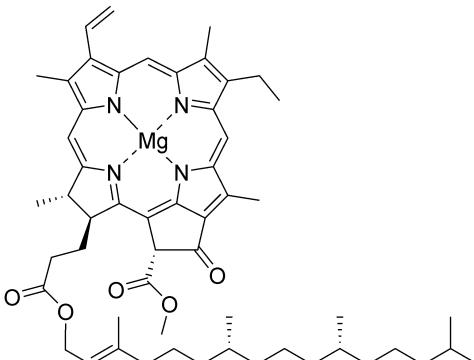
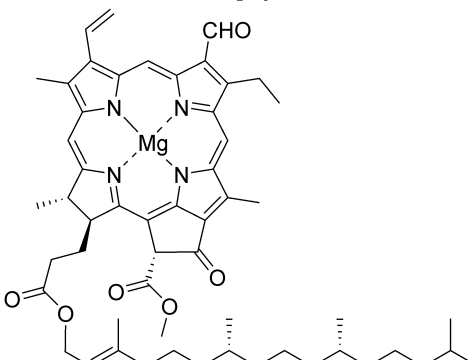
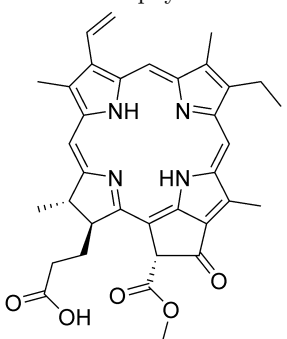
Continued on next page

Compound	$\hbar\omega$ (eV)	S (reduced)	τ_{LP} (ps)	τ_{UP} (ps)	References
 <p>H2TBP(CO₂Bu)</p>	0.14	0.11	2.1	296	76
 <p>ZnTBP(CO₂Bu)</p>	0.16	0.04	2.3	1760	76
 <p>H2TBP(CO₂Me)Ph</p>	0.16	0.16	2.1	103	77
 <p>ZnTBP(CO₂Me)Ph</p>					

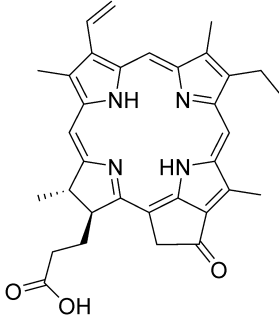
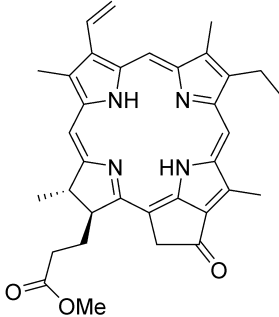
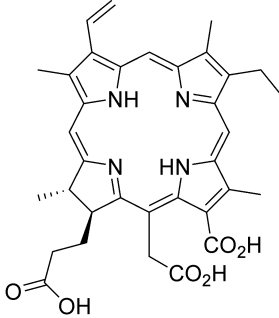
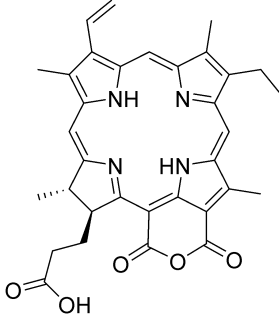
Continued on next page

Compound	$\hbar\omega$ (eV)	S (reduced)	τ_{LP} (ps)	τ_{UP} (ps)	References
ZnTBP(CO ₂ Me)Ph 	0.13	0.07	2.2	738	78
ZnTBP(CO ₂ Bu)Ph 	0.13	0.07	2.2	709	76
PdTBP(CO ₂ Bu)Ph 	0.16	0.21	2.2	55.7	76
C6F ₅ -Corrole 	0.16	0.16	2.2	98.1	78, 79
H ₂ Pc 	0.09	0.06	2.3	1797	80, 81

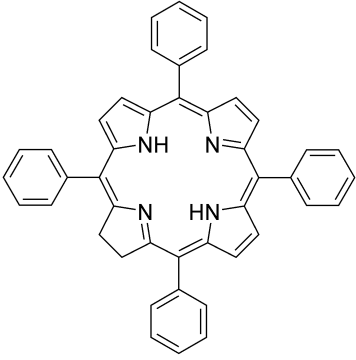
Continued on next page

Compound	$\hbar\omega$ (eV)	S (reduced)	τ_{LP} (ps)	τ_{UP} (ps)	References
 H2Pc(tBu)	0.10	0.06	2.3	1565	82
 chlorophyll a	0.14	0.06	2.2	900	83, 84
 chlorophyll b	0.16	0.03	2.3	2081	84, 85
 pheophorbide a	0.17	0.04	2.3	1438	86

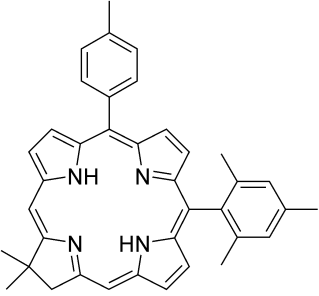
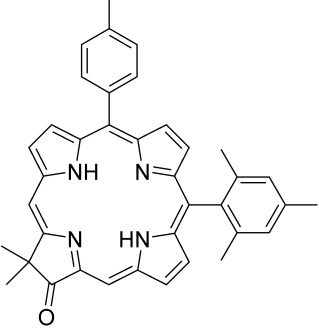
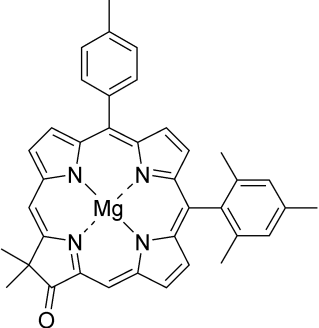
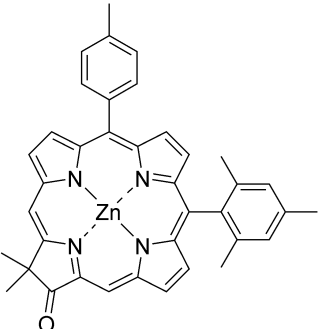
Continued on next page

Compound	$\hbar\omega$ (eV)	S (reduced)	τ_{LP} (ps)	τ_{UP} (ps)	References
 pyropheophorbide a	0.17	0.04	2.3	1669	87, 88
 pyropheophorbide a methyl ester	0.18	0.04	2.3	1,292	89, 90
 chlorin e6	0.17	0.03	2.4	3017934	91, 92
 purpurin 18	0.16	0.03	2.4	2,588	93, 94

Continued on next page

Compound	$\hbar\omega$ (eV)	S (reduced)	τ_{LP} (ps)	τ_{UP} (ps)	References
 H2TPC	0.17	0.03	2.4	2,556	95, 96

Continued on next page

Compound	$\hbar\omega$ (eV)	S (reduced)	τ_{LP} (ps)	τ_{UP} (ps)	References
 H2C-1	0.17	0.03	2.3	2,241	97, 98
 H2COxo-1	0.19	0.05	2.2	860	98
 MgCOxo-1	0.18	0.09	2.2	279	98
 ZnCOxo-1	0.17	0.06	2.2	676	98